and measured values from wind profiler at Pune[7] is made. The range of variation in the troposphere is 10^{-18} to 10^{-13} over Mumbai, $10^{-17.5}$ to $10^{-14.5}$ over Guwahati and that of measured values at Pune is 10^{-18} to 10^{-15} (Figure 5). The pattern of variation shows a gradual decrease from the surface to the upper troposphere for both the computed and measured values.

Unlike other atmospheric radars (rain radar or cloud radar), the wind profiling radars are mainly sensitive to radio-refractive index variation in the neutral atmosphere. This variation is caused by the small-scale atmospheric turbulence in the atmosphere. The refractive index structure parameter (C_n^2) is one of the basic variables of atmospheric turbulence calculation. The C_n^2 variation can be computed from the backscattered signal[13] and also from the known atmospheric parameters[12] of RS data. In the present communication, the annual and climatological variability of C_n^2 over two tropical stations, namely Mumbai and Guwahati has been analysed.

The mean C_n^2 values over the two stations are in the range 10^{-18} to 10^{-12} $m^{-2/3}$. The C_n^2 values are higher in the lower troposphere where both temperature and humidity gradients contribute to refractive index variation, and lower in the middle the upper troposphere where moisture gradient is negligible. The lowest values of C_n^2 are observed just below the tropopause region between 10 and 16 km over Guwahati and 10 and 13 km over Mumbai region. Over the two stations, in the summer (March–May) and southwest monsoon period, the high C_n^2 values in the lower troposphere extended even into the mid-tropospheric levels. As a coastal station, Mumbai shows higher values of C_n^2 at the surface and lower troposphere compared to Guwahati. This study would provide help system designers of wind profilers/ST radars in finalizing the radar parameters to achieve the required sensitivity for targeted height over that region.

1. Gage, K. S. and Balsley, B. B., Doppler radar probing of clear atmosphere. *Bull. Am. Meteorol. Soc*., 1978, **59**, 1074–1093.
2. Balsley, B. B. and Gage, K. S., On the use of radars for operational profiling. *Bull. Am. Meteorol. Soc*., 1982, **63**, 1009–1018.
3. VanZandt, T. E., Green, J. L., Gage, K. S. and Clark, W. L., Vertical profiles of reflectivity turbulence structure constant: comparison of observations by the Sunset Radar with a new theoretical model. *Radio Sci*., 1978, **13**, 819–829.
4. Sarkar, S. K., Pasricha, P. K., Dutta, H. N., Reddy, B. M. and Kulshrestha, S. M., Atlas of tropospheric radio propagation parameters over the Indian subcontinent. National Physical Laboratory, Delhi, 1985, pp. 200–239.
5. Ghosh, A. K., Sivakumar, V., Kishore Kumar, K. and Jain, A. R., VHF radar observations of atmospheric winds, associated shears and C_n^2 at a tropical location: interdependence and seasonal pattern. *Ann. Geophys*., 2001, **19**, 965–973.
6. Satheesan, K. and Krishna Murthy, B. V., Turbulence parameters in the tropical troposphere and lower stratosphere. *J. Geophys. Res. D*, 2002, **107**, 4002, doi:10.1029/2000JD000146.
7. Singh, N., Joshi, R. R., Chun, H. Y., Pant, G. B., Damle, S. H. and Vashishtha, R. D., Seasonal, annual and inter-annual features of turbulence parameters over the tropical station Pune (18°32′N, 73°51′E) observed with UHF wind profiler. *Ann. Geophys*., 2008, **26**, 3677–3692.
8. Hardy, K. R. and Katz, I., Probing the clear atmosphere with high power, high resolution radars. *Proc. IEEE*, 1969, **57**, 468–480.
9. Bufton, J. L., Correlation of microthermal turbulence with meteorological soundings in the troposphere. *J. Atmos. Sci*., 1973, **30**, 83–87.
10. Bufton, J. L., Comparison of vertical profile turbulence structure with stellar observations. *Appl. Opt*., 1973, **12**, 1785–1793.
11. Ehernberger, L. J., High altitude turbulence encountered by the supersonic YF-12A airplane. In Sixth Conference on Aerospace and Aeronautical Meteorology, American Meteorological Society, Boston, USA, 1974, pp. 305–312.
12. Tatarskii, V. I., The effects of the turbulent atmosphere on wave propagation. National Technical Information Service, Springfield, VA, USA, 1971, pp. 74–76.
13. Ottersten, H., Atmospheric structure and radar backscattering in clear air. *Radio Sci*., 1969, **4**, 1179–1193.

ACKNOWLEDGEMENTS. We thank the Department of Information Technology and the Society for Applied Microwave Electronics Engineering and Research, IIT Bombay for providing facilities to carry out this work. We also thank Dr K. P. Ray for useful suggestions and encouragement during this work; the University of Wyoming website for providing radiosonde data in the public domain, and the anonymous reviewers for suggestions that helped improve the paper.

Received 30 November 2012; revised accepted 11 January 2013

Run-off potential assessment over Indian landmass: a macro-scale hydrological modelling approach

S. P. Aggarwal, Vaibhav Garg*, Prasun K. Gupta, Bhaskar R. Nikam, Praveen K. Thakur and P. S. Roy

Indian Institute of Remote Sensing, Indian Space Research Organisation, 4, Kalidas Road, Dehradun 248 001, India

The evolution of land–atmosphere–ocean models has resulted in the need for hydrologic models applicable to large areas and river basins. Such developments offer new challenges and opportunities for hydrologists to understand the hydrologic response of areas as large as continents. In the present study, the ability of variable infiltration capacity (VIC) hydrological model has been studied to assess run-off potential and other hydrological components for entire India. VIC is a semi-distributed macroscale hydrological model designed to represent surface energy, hydrological fluxes and states at scales from large river basins to the entire globe. It is grid-based model which quanti-

*For correspondence. (e-mail: vaibhav@iirs.gov.in)

fies the dominant hydro-meteorological process taking place at the land surface–atmospheric interface. In the present study, the model was forced with 15 years daily precipitation, maximum and minimum air temperature at daily time-step on 25 × 25 km grid. The water balance of entire India has been studied and the model results on daily, monthly and annual timescales are discussed. It was found that the VIC model results in idealistic hydrology as it takes into account a large number of parameters influencing the process. It was realized that to study such a complex hydrological interaction between land surface and atmosphere over a large region, requires enormous data; in this regard remote sensing data may play an important role. The model can easily be adopted to get primarily information on water balance at any scale.

Keywords: Hydrological modelling, run-off potential, variable infiltration capacity, water balance.

HYDROLOGICAL modelling is a mathematical representation of natural processes which is generally defined largely by parameters and states, parameters being physical and generally time-variant descriptors of surface and subsurface characteristics, and states being fluxes and storages of water and energy that are propagated in time. Traditionally, hydrological models were developed to estimate or predict streamflow. Initially, a conceptual model, namely Stanford watershed model (SWM) was developed by Crawford and Linsley[1], which represented the spatially lumped run-off response of the land surface to precipitation. Till today, the derivatives of SWM remain in use such as the US National Weather Service River Forecast System and Hydrologic Simulation Package Fortran. The applicability of such models is limited as they are useful for simulation of streamflow only within the range of conditions for which they were developed. Also, the parameters of this type of models could not be easily related to physically measured quantities. Moreover, such models do not represent the effects of vegetation on evapotranspiration (ET) explicitly, nor do they perform the surface energy balance[2].

In the recent past, researchers have also developed models known as soil–vegetation–atmosphere transfer schemes (SVATS). These schemes have been explicitly developed to represent the land surface partitioning of net radiation into latent, sensible and ground heat fluxes in climate and weather forecast models. These models do consider the role of vegetation in the estimation of ET. Furthermore, they maintain surface energy balance by iterating on one or more effective temperatures[2]. However, SVATS generally emphasize on vertical/column processes such as extraction of soil moisture by vegetation, and feedback between vegetation, soil moisture and surface atmospheric conditions that control transpiration. These models usually do not consider horizontal complexity/spatial heterogeneity of soil and vegetation, and topography which control run-off generation[3,4].

The variable infiltration capacity (VIC) macroscale land surface hydrological model was also developed as a SVATS for general circulation models (GCMs) by Liang *et al.*[5]. Compared to other SVATS, it has various distinguished features such as the subgrid variability in soil moisture storage capacity as a spatial probability distribution, subgrid variability of land cover/land use (LULC) and drainage from a lower soil moisture zone (base flow) as a nonlinear recession[6,7]. Further details of the VIC model can be found in the literature[2,5,8,9]. The VIC model runs in various modes, namely energy balance, water balance and routing. In the present analysis, the two layers VIC (VIC-2L) model was run in water balance mode, driven by precipitation, and maximum temperature and minimum temperature at a daily time-step, for the entire Indian land mass. It has been applied to simulate the total daily run-off potential and ET for each grid cell independently. The set up of the VIC-2L model for the entire Indian region has been elaborated here. The model-generated long-term mean run-off potential was found to agree with Indian conditions to considerable accuracy.

India has been known for large variability in the availability of water resources. The country is endowed with almost all the important topographical features such as high mountains in the north, extensive plateaus, wide plains traversed by mighty rivers and ocean in the south which influence its climate.

These widely varying climatic conditions in conjunction with a range of topographic and soil properties lead to a complex water resources distribution over the country. Therefore, in the present study, the VIC-2L model has been established for entire India to analyse its water budget at 25 × 25 km grid (Figure 1). It was identified that 4707 grids lie on land mass and are to be run for analysis. The base map in Figure 1 is GTopo30 digital elevation model (DEM) (http://eros.usgs.gov/#/Find_Data/Products_and_Data_Available/GTOPO30), which has been used for elevation and slope parameters. In order to implement the VIC model, five main input files are required, namely forcing, soil parameter, vegetation parameter, vegetation library and global parameter file in ASCII format.

In the present study, as the model was employed in water balance mode, the meteorological parameters considered to force the model were daily precipitation, and daily minimum and maximum temperature. The 0.5° × 0.5° precipitation; and 1° × 1° minimum and maximum temperature gridded data of India Meteorological Department (IMD) have been procured for the period 1991–2005. For each grid, forcing files containing daily precipitation and minimum and maximum temperature from 1991 to 2005 have been generated.

According to Lohmann *et al.*[10,11], the representation of soil hydrology such as soil water storage, surface run-off generation and sub-surface drainage plays a critical role in the prediction of long-term water and energy balance.

The soil parameter file which describes the unique soil properties for each grid cell in the model domain in addition to several other variables is prepared. As mentioned above, VIC-2L has been adopted in the present analysis considering soil layers ($z1$, $z2$) of 0–300 and 300–1000 mm depth respectively. Hence, 02 layers of soil with 300 and 700 mm depth have been considered. The soil information, namely soil texture, percentage sand, percentage clay and bulk density (BD) corresponding to each layer depth has been extracted from Food and Agriculture Organization's (FAO) digitized soil map of the world at 1 : 5,000,000 scale and its database is shown in Figure 2 and Table 1.

To bridge the gap between rigid soil textural classes and heterogeneous nature of the soils, numerous pedotransfer functions (PTFs) have been developed[12–14]. The most commonly used lookup tables by land surface models and meteorological modelling applications are based on PTFs, which relate discrete soil types to measurable hydraulic parameters using regression equations derived from soil samples. In order to ensure consistency and add flexibility within soil types and hydraulic parameters, the saturated hydraulic conductivity (K_{sat}, cm/h) was derived using PTFs from Cosby *et al.*[14] which require only percentages of sand and clay. The maximum velocity of baseflow has been estimated by multiplying K_{sat} of each grid cell with its slope. However, the fraction of maximum soil moisture where nonlinear baseflow occurs is taken as 0.9 in the present study as it should be always greater than 0.5. The wilting point (wp, cm^3/cm^3) and field capacity (w, cm^3/cm^3) for the VIC model are described as a fraction of maximum moisture content at 15 and 1/3 bar tension respectively. Seventy per cent of w is taken as field capacity at critical point (w_{cr}, m/m). Initial moisture content of each layer $z1$ and $z2$ (*int. sm* $z1$, $z2$) can be computed as a depth in mm by multiplying w_{cr} by the thickness of the layer (m), and then multiplying by 1000. The maximum soil moisture for each soil layer depth (max sm $z1$, $z2$; m/m) is calculated by multiplying soil layer depth with its porosity (η). The fraction of w_{cr} (w_{cr} fract $z1$, $z2$) and *wp* (wp fract $z1$, $z2$) for each soil

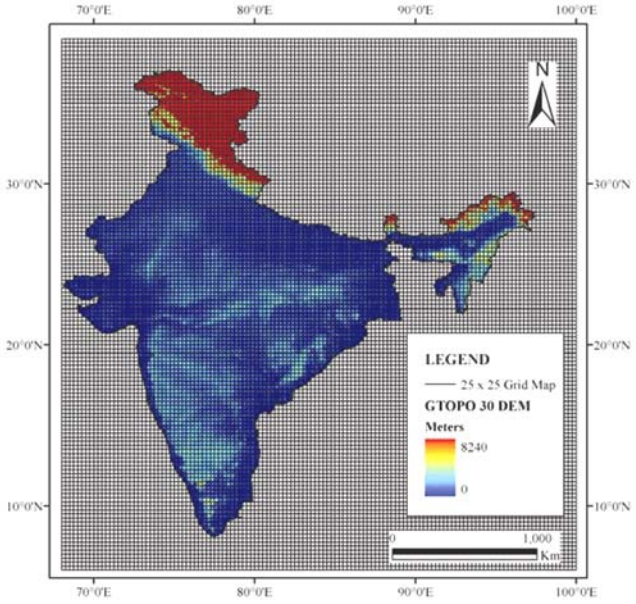

Figure 1. GTopo 30 digital elevation model map of India showing its location.

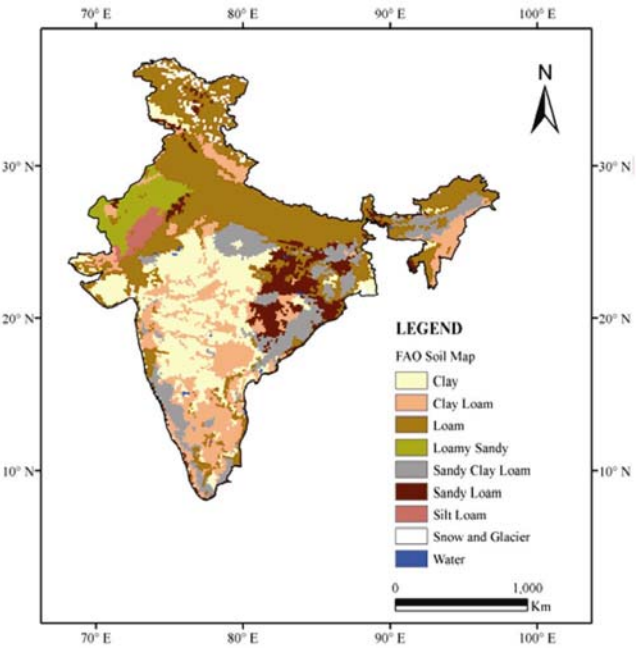

Figure 2. Soil map of India derived from FAO's digital soil map of the world.

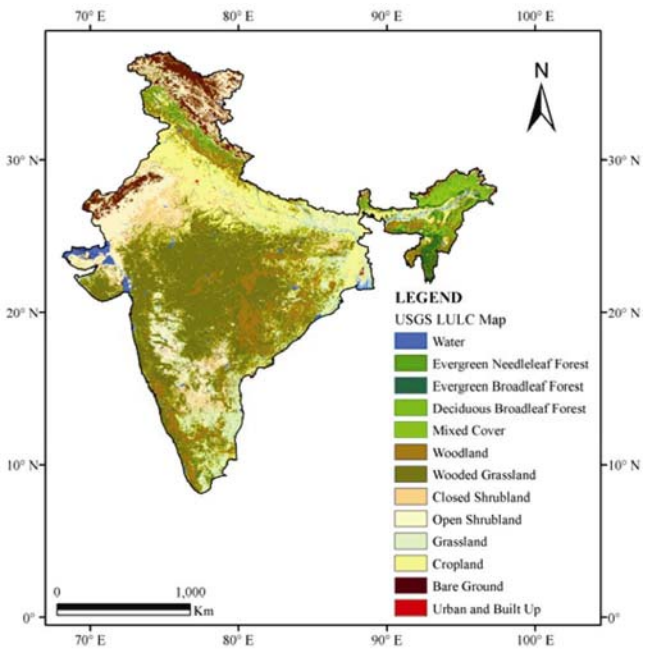

Figure 3. UMD land cover classification map of India.

Table 1. Soil hydraulic properties

Soil type	Sand (%)	Clay (%)	BD	w	wcr	int. moist z1	int. moist z2	wp	Porosity fraction (η)	Ksat	b	max. sm z1	max. sm z2	wcr fract z1	wcr fract z2	wp fract z1	wp fract z2	expt z1	expt z2
s	94.83	2.27	1.49	0.08	0.06	16.80	39.20	0.03	0.43	38.41	4.10	0.13	0.30	0.13	0.13	0.07	0.07	11.20	11.20
ls	85.23	6.53	1.52	0.15	0.11	31.50	73.50	0.06	0.42	10.87	3.99	0.13	0.29	0.25	0.25	0.14	0.14	10.98	10.98
sl	69.28	12.48	1.57	0.21	0.15	44.10	102.90	0.09	0.40	5.24	4.84	0.12	0.28	0.37	0.37	0.23	0.23	12.68	12.68
sil	19.28	17.11	1.42	0.32	0.22	67.20	156.80	0.12	0.46	3.96	3.79	0.14	0.32	0.49	0.49	0.26	0.26	10.58	10.58
si	4.50	8.30	1.28	0.28	0.20	58.80	137.20	0.08	0.52	8.59	3.05	0.16	0.36	0.38	0.38	0.15	0.15	9.10	9.10
l	41.00	20.69	1.49	0.29	0.20	60.90	142.10	0.14	0.43	1.97	5.30	0.13	0.30	0.47	0.47	0.33	0.33	13.60	13.60
scl	60.97	26.33	1.60	0.27	0.19	56.70	132.30	0.17	0.39	2.40	8.66	0.12	0.27	0.48	0.48	0.44	0.44	20.32	20.32
sicl	9.04	33.05	1.38	0.36	0.25	75.60	176.40	0.21	0.48	4.57	7.48	0.14	0.34	0.53	0.53	0.44	0.44	17.96	17.96
cl	30.08	33.46	1.43	0.34	0.24	71.40	166.60	0.21	0.46	1.77	8.02	0.14	0.32	0.52	0.52	0.46	0.46	19.04	19.04
sc	50.32	39.30	1.57	0.31	0.22	65.10	151.90	0.23	0.41	1.19	13.00	0.12	0.29	0.53	0.53	0.56	0.56	29.00	29.00
sic	8.18	44.58	1.35	0.37	0.26	77.70	181.30	0.25	0.49	2.95	9.76	0.15	0.34	0.53	0.53	0.51	0.51	22.52	22.52
c	24.71	52.46	1.39	0.36	0.25	75.60	176.40	0.27	0.47	3.18	12.28	0.14	0.33	0.54	0.54	0.57	0.57	27.56	27.56

s, Sand; ls, Loamy sand; sl, Loamy sandy; sil, Silty loamy; si, Silt; l, Loamy; scl, Sandy clay loamy; sicl, Silty clay loamy; cl, Clay loamy; sc, Sandy clay; sic, Silty clay; c, Clay.

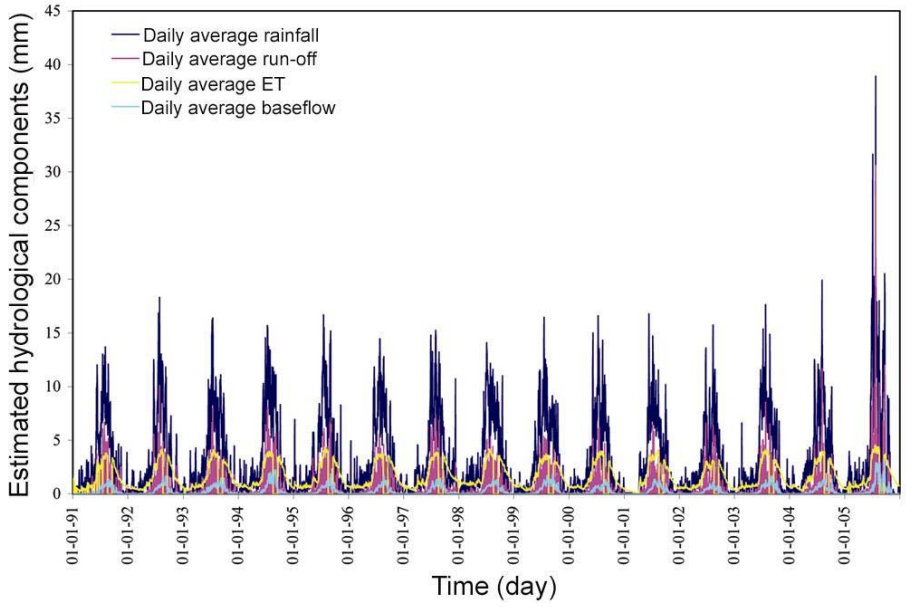

Figure 4. Daily time series of estimated run-off, baseflow and evapotranspiration (ET) average over entire India.

layer depth is calculated by multiplying w_{cr} and *wp* by corresponding soil depth and dividing by the respective max sm. The slope of the retention curve in log space (*b*) is calculated using Campbell's[13] relationship. The exponent (expt *z*1, *z*2) parameter is same as the exponent, *n*, in the Brooks–Corey relationship. It can be estimated using the expression 3 + 2**b* and the values should always be more than 3.0. The values of these parameters corresponding to the respective soil texture are provided in Table 1. All these parameters have been designated for each grid along with its longitude, latitude, median elevation, mean annual rainfall and initial soil moisture to initiate the model.

Both LULC and hydrology are linked with each other in a complex way at multiple spatial and temporal scales[15–24]. The changes in LULC alter the energy fluxes thereby affecting the climate, whereas climatic variability and change in turn affect the LULC patterns through the feedback mechanism[15,20,25–28]. A composite of these changes affects availability of water spatially and temporally. The vegetation parameter and vegetation library files were prepared from global land cover classification map generated by the University of Maryland (UMD), Department of Geography (Figure 3) at a 1 km nominal spatial resolution[29,30].

The vegetation parameter file defines the number of vegetation types in each grid cell, along with their fractional coverage, root depth and its fraction. The vegetation library file defines the different land-cover types allowed in the simulation and the corresponding influencing parameters, namely architectural resistance, minimum stomatal resistance, leaf-area index, shortwave albedo, vegetation roughness length and displacement height, trunk ratio and height at wind speed are measured. In this file, a flag has to be assigned to indicate whether or not the current vegetation type has an overstory. The values of these parameters corresponding to each LULC class are available in LDAS 8th database and MM5 Terrain dataset (http://ldas.gsfc.nasa.gov/nldas/NLDASmapveg.php).

The global parameter file is the main input file of the VIC model which sets simulation options, such as start/end dates and modes of operation, compiling the locations of the above prepared input files and directory which will store output files.

The above described methodology of setting up the VIC model has been well validated at basin scale by Dadhwal *et al.*[31] for Mahanadi. The results of the study, provided an impetus to carry out the daily hydrological simulation of the entire Indian land mass adopting VIC model for period from 1991 to 2005. The aforementioned five input files were prepared corresponding to each grid. The hydrological components such as potential run-off, baseflow and ET are determined at each grid and results are discussed at daily, monthly and yearly basis.

It was found that the estimated run-off is around 10.34% of rainfall, which usually holds for Indian conditions, if the average over the entire land mass (including arid and semi-arid regions) for the years under (comprised of dry and wet years) consideration is taken into account. The average run-off coefficient has been found to be 0.17 for monsoon season for entire India, including arid and semi-arid regions and the Rann of Kutch. The time-series plot of daily estimated run-off, baseflow and ET corresponding to daily rainfall is presented in Figure 4. The plot shows idealistic results as run-off, ET and

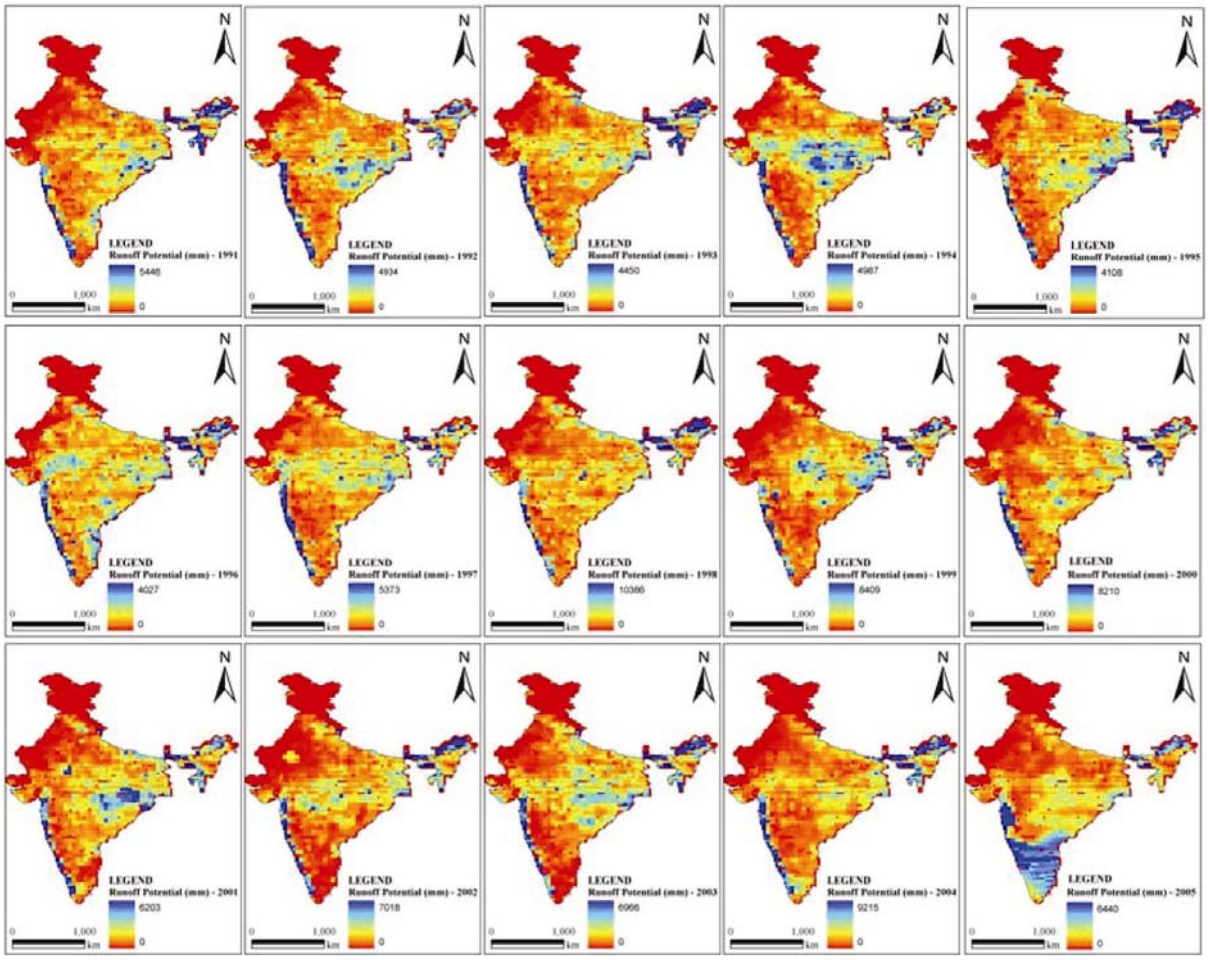

Figure 5. Spatio-temporal estimated run-off pattern maps of India for the years under consideration.

baseflow are following the usual pattern. It can be observed that the dry year 1991 shows somewhat high ET and less run-off, whereas the wet year 2005 is distinctly visible in the figure.

Figure 5 shows the temporal maps of spatial variation of estimated run-off. Again, one can notice dry year 1991 and wet year 2005 distinctly in these maps. It can also be noticed consistently that the Western Ghats falls in the high run-off potential region, which is in good agreement with the Indian condition. Similarly, central, eastern and northeastern India show high run-off, which is a visible effect of the Indian monsoon and regional terrain characteristics.

Moreover, the heavy floods in Odisha during 1994, 1995, 2001 and 2003 are easily identifiable (Department of Water Resources, Government of Odisha, http://www.dowrorissa.gov.in/HistoryofFLOOD/HistoryofFLOOD.pdf). The western states, especially Rajasthan, show low run-off potential as these belong to low-rainfall region (arid/semi-arid regions). However, regions falling in the higher reaches of northwest Himalayas show low run-off potential, as most of the area is covered under snow or glaciers, whose contribution has not been considered for run-off estimation in the present analysis.

As the main objective of the study was to obtain information on water balance of entire India, the spatio-temporal maps of estimated total of each hydrological component were also produced (Figure 6). These maps show perfect water balance for each year under consideration. ET is more or less the same every year. It can be noticed that as rainfall increases, run-off also increases. A time series plot of average of these components has also been prepared (Figure 7).

Finally, the monthly maps of run-off were prepared so that the effect of monsoon can be studied (Figure 8). At present only the maps corresponding to dry and wet years, i.e. 1991 and 2005 respectively, are presented. The effect of monsoon rain on run-off is visible during the monsoon season of both years. Moreover, the impact of the 25 July 2005 Mumbai flood on run-off is also distinctly evident in Figure 8. It can be concluded that macro-scale VIC model performs well even to study the national-level hydrology. The model results can be also used for long-term national-level planning.

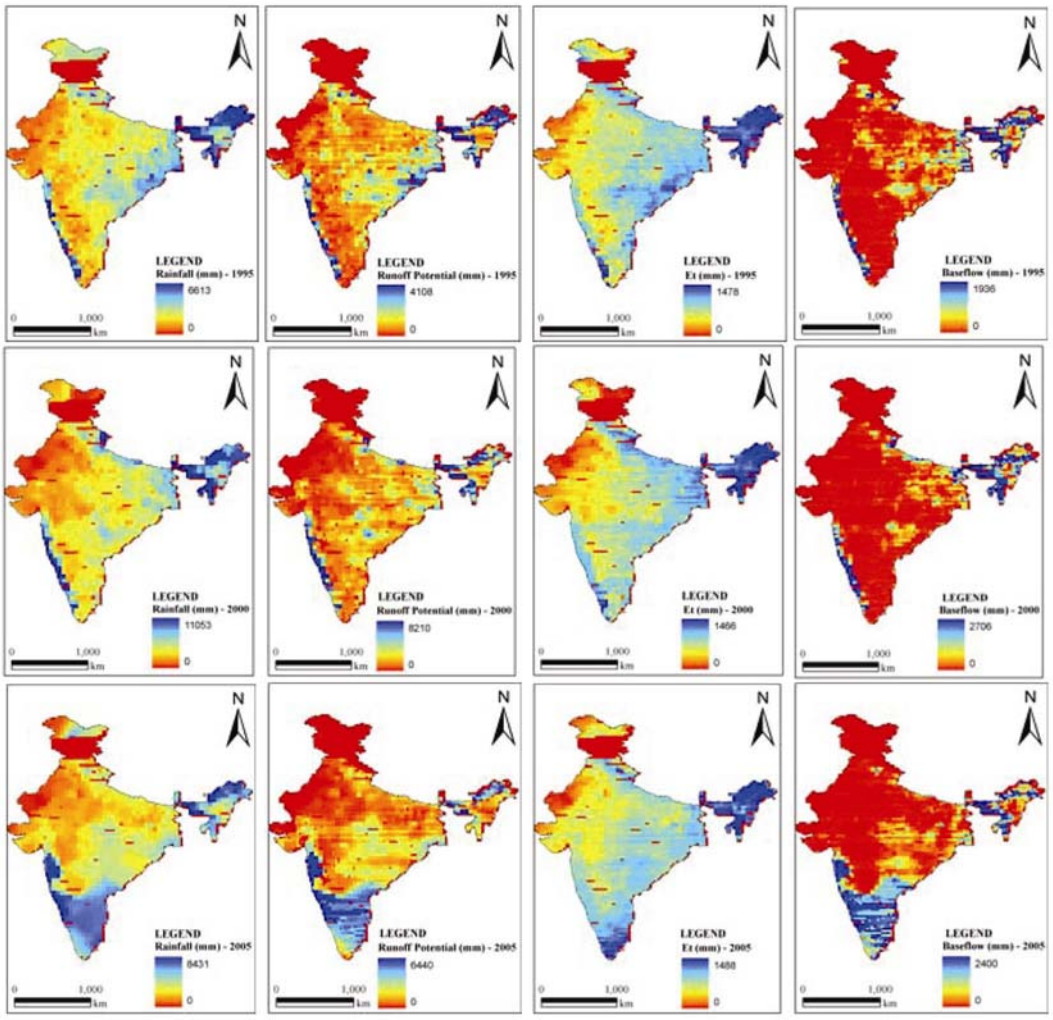

Figure 6. Estimated hydrological components for the years 1995, 2000 and 2005.

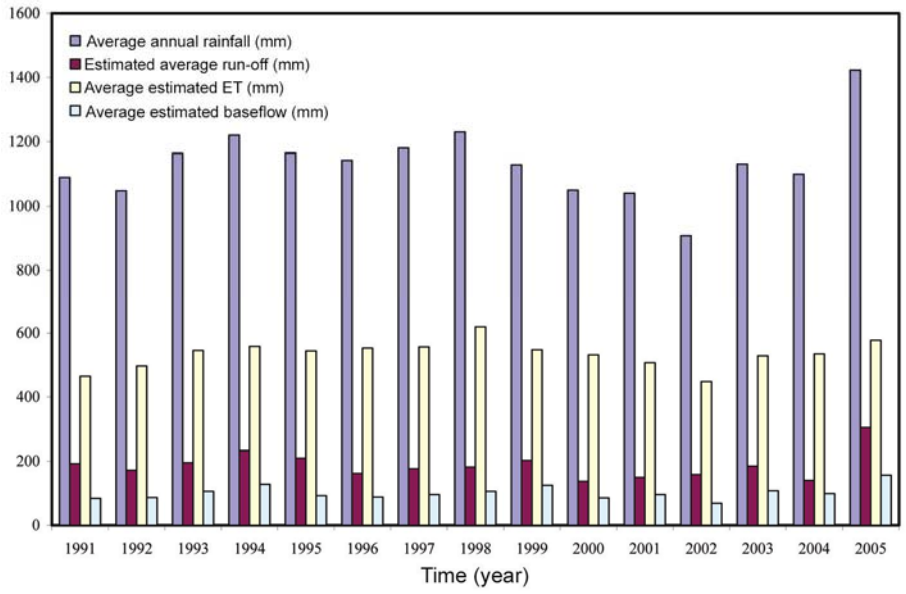

Figure 7. Time-series plot of average estimated hydrological components for each year under consideration.

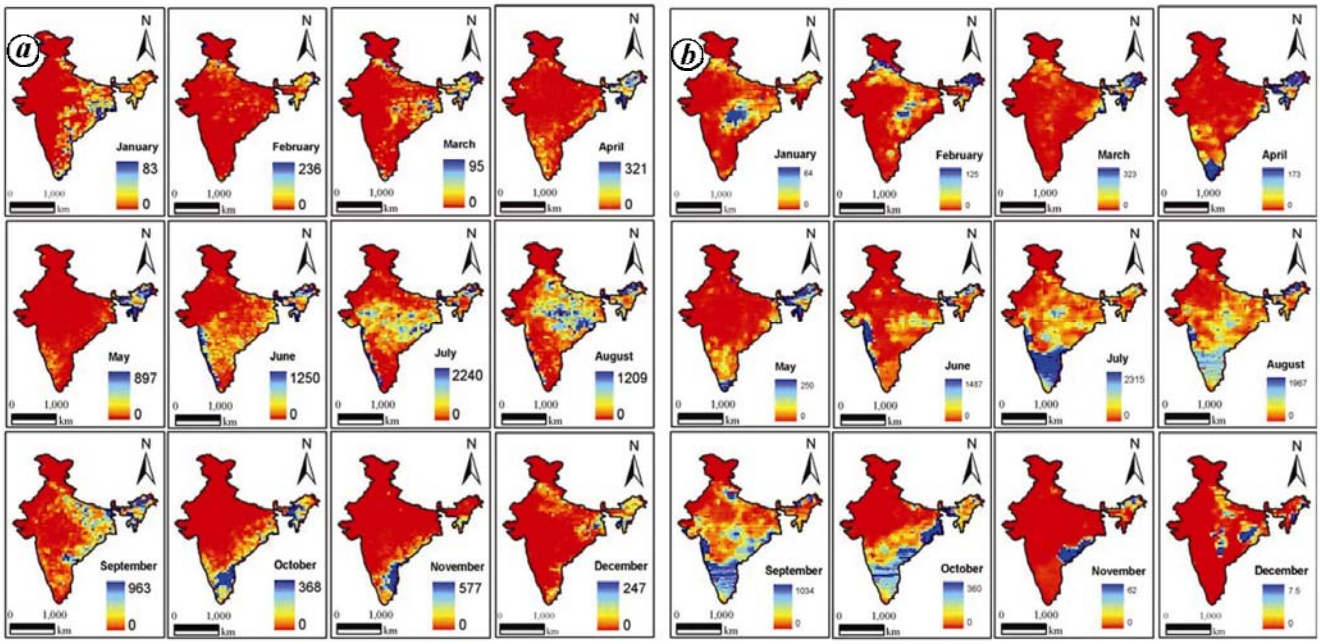

Figure 8. Monthly spatio-temporal variation of estimated run-off (mm). (***a***) Dry year 1991 and (***b***) Wet year 2005.

Table 2. Comparison of reported and estimated run-off in major basins of India

Basin	Estimated run-off (m ha-m)				
	Rao[32]	Chaturvedi[33]	Zade *et al.*[34]	Gupta and Panigrahy[35]	Present study
Indus	7.70	4.20	18.50	10.00	1.17
Ganga	55.00	49.30	58.93	37.60	83.40
Narmada + Luni and Ghaggar	8.80	7.10	18.27	11.10	18.04
Brahmaputra	59.70	51.00	48.83	23.30	27.19
Mahanadi	11.50	7.50	20.64	15.30	9.73
Godavari	11.50	10.50	20.57	13.20	7.17
Western Ghats + Cauvery	24.60	–	–	15.90	17.03
Krishna	5.80	6.70	17.90	8.50	6.30
Pennar	2.50	0.30	–	7.90	3.07
Total	187.10	136.60	203.64	142.80	173.10

A comparative analysis at basin scale has also been carried out to validate the results obtained in the present study for 2004 with observations reported in the literature[32–35] (Table 2). Zade *et al.*[34] and Gupta and Panigrahy[35] adopted the Natural Resources Conservation Services Curve Number (formerly known as Soil Conservation Services Curve Number) approach for analysis of run-off pattern for all major basins in India for 2004. A close agreement between the reported and estimated run-off values in most of the basins has been found, except Indus and Ganga basins. In the Indus basin major contribution to surface run-off comes from snow melt; however, snow grids have been neglected in the present study, which might have attributed to difference in the estimates. Therefore, the difference might have attributed as snow melt contribution has not been calculated, in this analysis. In the case of Ganga basin, average annual flow of 52.5 m ha-m at Farraka has been reported[36,37]. However, in the present study the run-off potential has been estimated considering the virgin basin (excluding storage in Ramganga, Tehri, Rana Pratap Sagar, Parbati, Matatila, Dhauliganga, Damodar Valley Cooperation reservoirs constructed on tributaries of the Ganga and water diverted for major irrigation projects, namely Ganga canal systems and Yamuna canal systems to irrigate most of the Indo-Gangetic Plain). Moreover, the present simulation has been carried out at a national scale. The effect of unique geophysical properties of each basin on its run-off potential may have nullified at this spatial scale. Therefore, the values run-off potential reported in Table 2 by and large comparable with each other. The estimation of run-off potential/discharge of an individual basin

incorporating its unique characteristics in terms of storage, diversion and usage may be the future scope of this communication.

With the geographical area of the country being 328.73 m ha, the calculated run-off coefficient is 0.43 for 2004, which compares well with those of Zade *et al.*[34] (0.50) and Gupta and Panigrahy[35] (0.35).

The macro-scale VIC-2L hydrological model has been investigated to study hydrology and its components for the entire Indian land mass. It was found that the model results satisfy the water balance of the entire country for every year under consideration. Such studies may prove to be useful for broad water resources and irrigation planning. It also provides information on the direction and magnitude of run-off change and insights into which variables are most significant for these changes. It may provide vital information about flood control too. Moreover, it was realized that the model can be used to study the impact of future climate change on hydrological regime of river basin, as it is compatible with RCM and GCM outputs. So, the future state of the water resources can also be assessed, which may help decision-makers evaluate mitigation and adaptation strategies under different climate scenarios, as well as to support policies about water allocations between various sectors such as agriculture, ecosystems, domestic and industry.

The VIC model requires a large number of land surface and atmospheric variables influencing hydrology. To retrieve these parameters over a large area, remote sensing data can play an important role. In the present study, the available global dataset on LULC, soil and their corresponding parameters was used, whereas there is an urgent need to develop such datasets at fine scale specifically for the nation.

1. Crawford, N. H. and Linsley, R. K., Computation of a synthetic streamflow record on a digital computer. *Int. Assoc. Sci. Hydrol. Publ.*, 1960, **51**, 526–538.
2. Lettenmaier, D. P., Present and future of modeling global environmental change: toward integrated modeling. In *Macroscale Hydrology: Challenges and Opportunities* (eds Matsuno, T. and Kida, H.), 2001, pp. 111–136.
3. Wood, E. F., Global scale hydrology: advances in land surface modeling. *Rev. Geophys. Suppl.*, 1991, **29**, 193–201.
4. Abdulla, F. A., Lettenmaier, D. P., Wood, E. F. and Smith, J. A., Application of a macroscale hydrologic model to estimate the water balance of the Arkansas-Red river basin. *J. Geophys. Res. D*, 1996, **101**, 7449–7459.
5. Liang, X., Lattenmaier, D. P., Wood, E. F. and Burgess, S. J., A simple hydrologically based model of land surface, water, and energy flux for general circulation models. *J. Geophys. Res. D*, 1994, **99**, 14415–14428.
6. Zhao, R. J., Zhang, Y. L., Fang, L. R., LIu, X. R. and Zhang, Q. S., The Xinanjiang model. In *Hydrological Forecasting Proceedings Oxford Symposium*, International Association of Hydrological Sciences, 1980, vol. 129, pp. 351–356.
7. Dumenil, L. and Todini, E., A rainfall–run-off scheme for use in the Hamburg climate model. In *Advances in Theoretical Hydrology, A Tribute to James Dooge* (ed. O'Kane, P.), European Geophysical Society Series on Hydrological Sciences, 1992, vol. 1, pp. 129–157.
8. Liang, X., A two-layer variable infiltration capacity land surface representation for general circulation models. Water Resource. Series, TR140, University of Washington, Seattle, 1994.
9. Liang, X., Lettenmaier, D. P. and Wood, E. F., One-dimensional statistical dynamic representation of subgrid spatial variability of precipitation in the two-layer variable infiltration capacity model. *J. Geophys. Res. D*, 1996, **101**, 21403–21422.
10. Lohmann, D. E., Raschke, N. B. and Lettenmaier, D. P., Regional scale hydrology: I. Formulation of the VIC-2L model coupled to a routing model. *Hydrol. Sci. J.*, 1998, **43**, 131–141.
11. Lohmann, D. E., Raschke, N. B. and Lettenmaier, D. P., Regional scale hydrology: II. application of the VIC-2L model to the Weser river, Germany. *Hydrol. Sci. J.*, 1998, **43**, 143–158.
12. Brooks, R. H. and Corey, A. T., Hydraulic properties of porous media. *Hydrol. Pap.*, 1964, **3**.
13. Campbell, G. S., A simple method for determining unsaturated conductivity from moisture retention data. *Soil Sci.*, 1974, **117**, 311–314.
14. Cosby, B. J., Hornberger, G. M., Clapp, R. B. and Ginn, T. R., A statistical exploration of the relationships of soil moisture characteristics to the physical properties of soils. *Water Resour. Res.*, 1984, **20**, 682–690.
15. Bosch, J. M. and Hewlett, J. D., A review of catchment experiments to determine the effect of vegetation changes on water yield and evapotranspiration. *J. Hydrol.*, 1982, **55**, 3–23.
16. Stednick, J. D., Monitoring the effects of timber harvest on annual water yield. *J. Hydrol.*, 1996, **176**, 79–95.
17. Matheussen, B., Kirschbaum, R. L., Goodman, I. A., O'Donnell, G. M. and Lettenmaier, D. P., Effects of land cover change on streamflow in interior Columbia River Basin (USA and Canada). *Hydrol. Process.*, 2000, **14**, 867–885.
18. Foley, J. A., Kucharik, C. J., Twine, T. E. and Coe, M. T., Land use, land cover, and climate change across the Mississippi basin: impacts on selected land and water resources. In *Ecosystems and Land Use Change* (eds DeFries, R., Asner, G. and Houghton, R.), Geophysical Monograph Series 153, American Geophysical Union, Washington, DC, 2004, pp. 249–261.
19. Gosain, A. K., Rao, S. and Basuray, D., Climate change impact assessment on hydrology of Indian river basins. *Curr. Sci.*, 2006, **90**, 346–353.
20. Gao, Z., Xhang, Z. and Zhang, X., Responses of water yield to changes in vegetation at a temporal scale. *Front. For. China*, 2009, **4**, 53–59.
21. Ma, X., Xu, J., Luo, Y., Aggarwal, S. P. and Li, J., Response of hydrological processes to land-cover and climate changes in Kejie watershed, south-west China. *Hydrol. Proc.*, 2009, **23**, 1179–1191.
22. Petchprayoon, P., Blanken, P. D., Ekkawatpanit, C. and Hussein, K., Hydrological impacts of land use/land cover change in a large river basin in central–northern Thailand. *Int. J. Climatol.*, 2010, doi: 10.1002/joc.2131
23. Schilling, K. E., Chan, K. S., Liu, H. and Zhang, Y. K. Quantifying the effect of land use land cover change on increasing discharge in the Upper Mississippi River. *J. Hydrol.*, 2010, **387**, 343–345.
24. Homdee, T., Pongput, K. and Kanae, S., Impacts of land cover changes on hydrologic responses: a case study of Chi River Basin, Thailand. *Ann. J. Hydraul. Eng., JSCE*, 2011, **55**, S31–S36.
25. Sahin, V. and Hall, M. J., The effects of afforestation and deforestation on water yields. *J. Hydrol.*, 1996, **178**, 293–309.
26. Chase, T. N., Pielke Sr, R. A., Kittel, T. G. F., Nemani, R. R. and Running, S. W., Simulated impacts of historical land cover changes on global climate in northern winter. *Clim. Dyn.*, 2000, **16**, 93–105.

27. DeFries, R. and Eshleman, K. N., Land-use change and hydrologic processes: a major focus for the future. *Hydrol. Proc.*, 2004, **18**, 2183–2186.
28. Piao, S., Friedlingstein, P., Ciais, P., de Noblet-Ducoudré, N., Labat, D. and Zaehle, S., Changes in climate and land use have a larger direct impact than rising CO_2 on global river run-off trends. *Proc. Natl. Acad. Sci. USA*, 2007, **104**, 15242–15247.
29. Hansen, M., DeFries, R., Townshend, J. R. G. and Sohlberg, R., UMD global land cover classification, 1 Kilometer, 1.0, Department of Geography, University of Maryland, College Park, Maryland, 1998.
30. Hansen, M., DeFries, R., Townshend, J. R. G. and Sohlberg, R., Global land cover classification at 1km resolution using a decision tree classifier. *Int. J. Remote Sensing*, 2000, **21**, 1331–1365.
31. Dadhwal, V. K., Aggarwal, S. P. and Misra, N., Hydrological simulation of Mahanadi River basin and impact of landuse/landcover change on surface runoff using a macro scale hydrological model. In International Society for Photogrammetry and Remote Sensing (ISPRS) TC VII Symposium – 100 years ISPRS (eds Wagner, W. and Szekely, B.), Vienna, Austria, 5–7 July 2010, ISPRS, vol. XXXVIII, Part 7B, pp. 165–170.
32. Rao, A. L., *India's Water Wealth. Its Assessment, Uses and Projections*, Orient Longman Limited, 1975.
33. Chaturvedi, M. C., *Second India Studies: Water*, Macmillan Co. India Ltd, New Delhi, 1976, pp. 12–22.
34. Zade, M., Ray, S. S., Dutta, S. and Panigrahy, S., Analysis of run-off pattern for all major basins of India derived using remote sensing data. *Curr. Sci.*, 2005, **88**, 1301–1305.
35. Gupta, P. K. and Panigrahy, S., Geo-spatial modeling of run-off of large land mass: analysis, approach and results for major river basins of India. In *Int. Arch. Photogramm., Remote Sensing and Spatial Inform. Sci.*, 2008, **XXXVII**, pp. 63–68.
36. Jain, S. K., Agarwal, P. K. and Singh, V. P., Hydrology and Water Resources of India. Water Science and Technology Library Series, Springer, The Netherlands, 2007, vol. 57.
37. CWC, *Integrated Hydrological Data Book (Non-Classified River Basins)*, Hydrological Data Directorate, Information System Organisation, Water Planning & Projects Wing, Central Water Commission, Government of India, 2012.

ACKNOWLEDGEMENTS. This work was carried out under the technology development project of Indian Space Research Organisation. We thank IMD for providing daily gridded data on rainfall and temperature and the anonymous reviewer and editors for their valuable comments and suggestions, and the VIC hydrological model team for their help.

Received 29 May 2012; revised accepted 10 January 2013

Ayurvedic formulations as therapeutic radioprotectors: preclinical studies on Brahma Rasayana and Chyavanaprash

Menon Aditya and C. K. K. Nair*

Pushpagiri Institute of Medical Sciences and Research Centre, Thiruvalla 689 101, India

Exposure to ionizing radiation reduces the cellular antioxidants and causes damage to genomic DNA. In the mammalian system, this results in various radiation syndromes depending on the radiation dose. Commercially available ayurvedic formulations, Brahma Rasayana (BRM) and Chyavanaprash (CHM) were analysed for their ability to restore the cellular antioxidant status and enhance the repair of radiation-induced DNA damages. The antioxidant status in various tissues of mice was restored when these formulations were orally administered, following whole-body exposure to gamma radiation. Administration of these formulations to 4 Gy whole-body gamma-irradiated mice resulted in faster cellular DNA repair, as revealed from the increased cellular repair index and decrease in the formation of micronucleus. This work suggests the possibility of using BRM or CHM as a therapeutic radioprotector during unplanned, accidental ionizing radiation exposure scenario.

Keywords: Antioxidant, Brahma Rasayana, cellular repair index, Chyavanaprash, DNA damage.

IONIZING radiation and radioisotopes have been used for various diagnostic, therapeutic, industrial and other applications such as military purposes, agricultural crop improvement, generation of nuclear power, etc. Personnel manning the radiation sources are often subjected to low levels of radiation and high dose exposure to radiation may occur due to accidents and during nuclear warfare[1].

There is a need to understand the mechanism of radiation damages and its prevention by effective nontoxic drugs. Agents which reduce the radiation-induced free-radical-mediated damages and enhance the cellular repair and recovery processes are called radioprotectors[2]. Development of novel and effective non-toxic radioprotectors is of considerable interest for application in defence (nuclear wars), nuclear industries, radiation accidents, space flight, etc., besides playing an important role in the protection of normal tissues during radiotherapy of tumours[3]. So far, no appropriate radioprotectors are available for practical applications with acceptable toxicity in the clinical situations. Amifostine, the only FDA-approved and clinically accepted radioprotector[4], is of limited utility due to its severe side effects at clinically

*For correspondence. (e-mail: ckknair@yahoo.com)